OPEN ACCESS Freely available online

PLoS one

Evaluation of the Efficacy and Safety of Rivaroxaban Using a Computer Model for Blood Coagulation

Rolf Burghaus[1], Katrin Coboeken[2], Thomas Gaub[2], Lars Kuepfer[2], Anke Sensse[3], Hans-Ulrich Siegmund[2], Wolfgang Weiss[2], Wolfgang Mueck[1], Joerg Lippert[2]*

1 Bayer Schering Pharma AG, Wuppertal, Germany, **2** Bayer Technology Services GmbH, Leverkusen, Germany, **3** Bayer Schering Pharma AG, Berlin, Germany

Abstract

Rivaroxaban is an oral, direct Factor Xa inhibitor approved in the European Union and several other countries for the prevention of venous thromboembolism in adult patients undergoing elective hip or knee replacement surgery and is in advanced clinical development for the treatment of thromboembolic disorders. Its mechanism of action is antithrombin independent and differs from that of other anticoagulants, such as warfarin (a vitamin K antagonist), enoxaparin (an indirect thrombin/Factor Xa inhibitor) and dabigatran (a direct thrombin inhibitor). A blood coagulation computer model has been developed, based on several published models and preclinical and clinical data. Unlike previous models, the current model takes into account both the intrinsic and extrinsic pathways of the coagulation cascade, and possesses some unique features, including a blood flow component and a portfolio of drug action mechanisms. This study aimed to use the model to compare the mechanism of action of rivaroxaban with that of warfarin, and to evaluate the efficacy and safety of different rivaroxaban doses with other anticoagulants included in the model. Rather than reproducing known standard clinical measurements, such as the prothrombin time and activated partial thromboplastin time clotting tests, the anticoagulant benchmarking was based on a simulation of physiologically plausible clotting scenarios. Compared with warfarin, rivaroxaban showed a favourable sensitivity for tissue factor concentration inducing clotting, and a steep concentration–effect relationship, rapidly flattening towards higher inhibitor concentrations, both suggesting a broad therapeutic window. The predicted dosing window is highly accordant with the final dose recommendation based upon extensive clinical studies.

Citation: Burghaus R, Coboeken K, Gaub T, Kuepfer L, Sensse A, et al. (2011) Evaluation of the Efficacy and Safety of Rivaroxaban Using a Computer Model for Blood Coagulation. PLoS ONE 6(4): e17626. doi:10.1371/journal.pone.0017626

Editor: Vladimir N. Uversky, University of South Florida College of Medicine, United States of America

Received November 4, 2010; **Accepted** February 3, 2011; **Published** April 22, 2011

Funding: This analysis was supported by Bayer Schering Pharma AG. The funders supplied clinical and preclinical data for the purpose of this study and supported the generation of the manuscript. Because the authors are employed by the funders, the funders did play a role in study design, data collection and analysis, decision to publish, and preparation of the manuscript.

Competing Interests: All authors are Bayer AG subsidiary employees and own stocks of Bayer AG. This does not alter the authors' adherence to all the PLoS ONE policies on sharing data and materials.

* E-mail: joerg.lippert@bayer.com

Introduction

The blood coagulation cascade is a complex process, involving both an intrinsic and an extrinsic pathway (Figure 1) [1]. The different classes of anticoagulant drugs currently on the market or in clinical development target different factors within the coagulation cascade (Figure 1). The most interesting new classes of anticoagulants include the direct thrombin inhibitors and the Factor Xa inhibitors (direct or indirect).

Rivaroxaban is an oral, direct Factor Xa inhibitor approved in more than 100 countries worldwide, including the European Union and Canada, for the prevention of venous thromboembolism after elective hip or knee replacement surgery in adult patients, and is in advanced clinical development for the treatment of thromboembolic disorders. Rivaroxaban only targets one factor within the coagulation cascade, Factor Xa, and its mechanism of action is antithrombin (AT) independent [2,3]. This mechanism of action is different from that of other anticoagulants that have been or are currently used in clinical practice, such as warfarin (a vitamin K antagonist) [4], enoxaparin (an indirect thrombin/Factor Xa inhibitor) [5,6], ximelagatran (now withdrawn) [7] and dabigatran (direct thrombin inhibitors) [8].

A computer model for blood coagulation has been developed, based on several published models [9–14]. In contrast to these previous models, the one presented here takes into account both the intrinsic and extrinsic pathways of the coagulation cascade and possesses some unique features that were not included in these earlier models, such as a blood flow component and a portfolio of drug action mechanisms based on their physicochemical properties and pharmacokinetic profiles. The aim of this study was to use this model to evaluate the efficacy and safety of different doses of rivaroxaban compared with other anticoagulants, thereby estimating a therapeutic window for rivaroxaban.

The model was built to cover several aspects of the coagulation cascade, including the extrinsic pathway (initiated with the triggering of tissue factor [TF]), the intrinsic pathway (initiated with activation of Factor XII [Factor XIIa]) and the common pathways leading to fibrin generation via thrombin generation. Additional features were also included: inhibition via the TF pathway inhibitor or via AT, and the fact that *in vivo* coagulation is affected by blood flow, which leads to an exchange of proteins between the clot and the fresh blood pool. The action of calcium ions (within membrane-bound enzyme complexes, e.g. the prothrombinase complex) were indirectly included in the rate

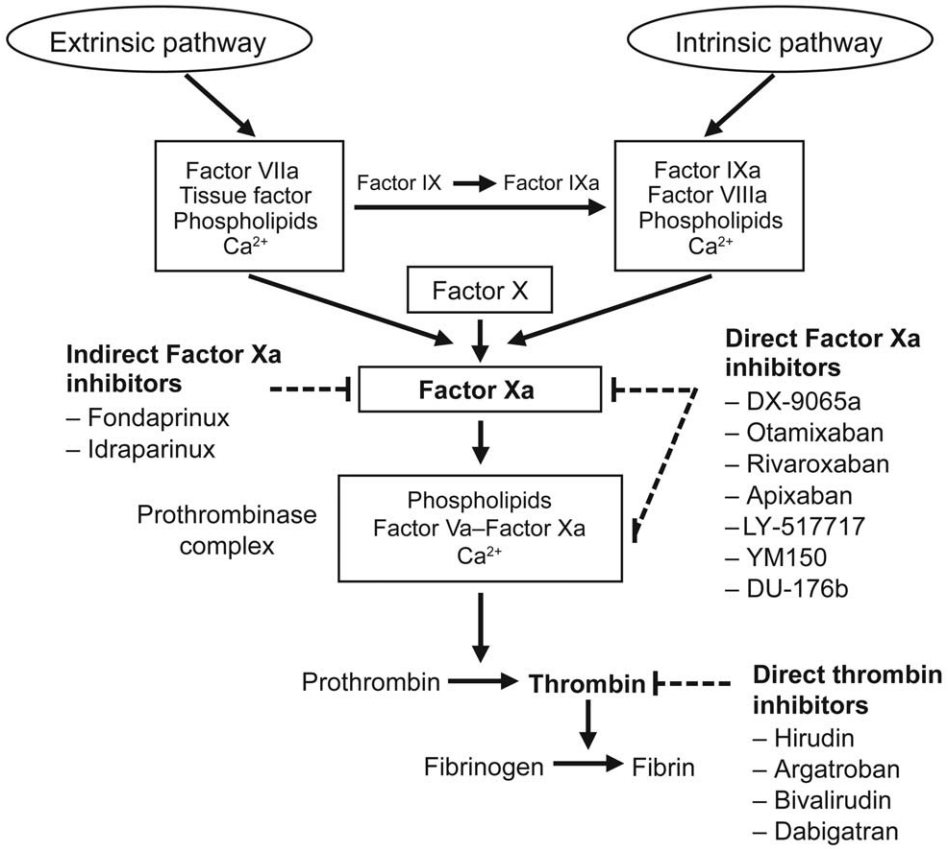

Figure 1. Targets for anticoagulant drugs in the coagulation pathway [57].
doi:10.1371/journal.pone.0017626.g001

constants and kinetic parameters, and phospholipid membrane-binding sites were directly included in the model kinetics. A portfolio of drug action mechanisms and pharmacokinetic profiles was also included in the model: rivaroxaban and DX-9065a (direct Factor Xa inhibitors), warfarin, enoxaparin and ximelagatran. The model was adjusted to accurately represent both preclinical information, such as directly measured dissociation constants, and clinical measurements such as the common clotting tests, prothrombin time (PT) and activated partial thromboplastin time (aPTT). Some additional aspects of the coagulation cascade will be developed in further improvements to the model, including: thrombocytes and their action; fibrinolysis and spatial thrombus properties.

This computer model was used to assess the efficacy and safety of rivaroxaban compared with that of other anticoagulants included in the model, by using physiologically plausible clotting scenarios with presumably high relevance for bleeding as well as thrombosis events. The computer model was subsequently applied to the modelling of the therapeutic window of rivaroxaban by comparing the inhibitory effect of all anticoagulants in these virtual clotting scenarios, which were not feasible with laboratory *in vitro* test systems.

Methods

Structural properties of the model

The program package MoBi® (Bayer Technology Services, Leverkusen, Germany) [15] was used as the software platform. The structural properties of the model represent qualitative knowledge about the coagulation processes. This is exemplified by the cleavage and activation of prothrombin (Factor II) to thrombin (Factor IIa) by Factor Xa. This reaction is included in the model to take into account both the stoichiometric part:

$$\text{Factor II} \rightarrow \text{Factor IIa} \tag{1}$$

and the kinetics part:

$$\text{k16} \times \text{Factor Xa} \times \text{Factor II} \tag{2}$$

(see: Appendix S1, Reaction R9)

Equation 1 represents the one-to-one (stoichiometric) conversion of Factor II to Factor IIa (prothrombin to thrombin). Equation 2 describes the kinetic law governing the rate of conversion: it is proportional to the concentrations of Factor Xa, Factor II, with k16 being the kinetic constant. Kinetic parameters and initial conditions (concentrations) represent the quantitative information about the coagulation system and take into account the impact of the different study drugs (see: Appendix S2 and Appendix S3). Kinetic equations are given according to standard mass action law convention.

The coagulation model

Individual factors and interactions were classified using the well-characterized extrinsic or intrinsic pathways, because the model was constructed to represent the typical in vitro tests used for investigating the extrinsic and intrinsic processes (PT and aPTT, respectively) in one unified computational representation. Transport reactions taking into account the blood flow were then

incorporated, so that the model was more closely related to the physiological in vivo setting.

The extrinsic core of the model was adapted from the model by Hockin et al. [10] and consists of 32 reactions (see: Appendix S1, reactions named with R and number). It covers all relevant interactions and factors, from the triggering of the cascade by TF, to Factor II (prothrombin) activation and Factor IIa (thrombin) formation. The PT test best assesses coagulation activity in the extrinsic pathway.

The intrinsic pathway was adapted from the model published by Kogan et al. [11] and consists of the reactions listed in Appendix S1 containing rate constants starting with 'Kog' (at the end of the appendix). It covers all relevant interactions and factors leading from Factor XIIa to Factor Xa. The aPTT test best assesses coagulation activity in the intrinsic pathway.

Further model extensions were taken from the model developed by Anand et al. [14]. A feedback loop for the activation of Factor XI and a reaction representing the cleavage of fibrinogen (RI), also introduced by Kogan et al. [11,16] and kinetic data taken from Stevens et al. [16] were added to the original model to define two independent thresholds for thrombus formation – one based on Factor IIa and the other on the fibrinogen cleavage product (named 'Ia' in the model and being used as a representation of fibrin formation) concentration, respectively.

The protein C/S system and the coagulation factor adsorption reactions to lipids were developed on the basis of the model published by Bungay et al. [9] and by Kuharsky and Fogelson [13]. In addition to reactions published by these authors, the protein C/S model part was extended by us with further reactions that reflect additional inactivation paths (see: Appendix S1, reaction names starting with 'RBu' containing extra letters appended to the number). The integration of phospholipid vesicles led to a set of adsorption reactions (see: Appendix S1, reaction names starting with 'Rad'), but we also needed to duplicate several reactions to account for the option that several of the components might react either when bound to phospholipids or when being dissolved (see: Appendix S1, reaction names of the scheme 'R' number 'd'). The species 'PhosphoLipid' represents protein-binding sites on phospholipid vesicles. Bungay et al. use an average of 100 phospholipid molecules per site, but our model was set to 333 molecules per site, being of the same size as published experimental values [17].

Additional coagulation factor inhibition reactions were introduced based on published rate constants [18–23]. The rate constant for the inhibitor AT (ATIII), which was in the upper

Table 1. Regimens for rivaroxaban, warfarin, ximelagatran, DX-9065a and enoxaparin included in the model.

Rivaroxaban		Warfarin		Ximelagatran		DX-9065a		Enoxaparin	
Dose (mg)	**Plasma level (μg/l)**	**Dose (INR)**	**Plasma level**	**Dose (mg)**	**Plasma level (μM)**	**Dose**	**Plasma level (μg/l)**	**Dose (mg s.c.)**	**Plasma level (mg/l)**
5 OD	C_{max} 60.98	1.5		24 BD	C_{max} 0.21	IV infusion	100	20 OD	C_{max} 1.79
	C_{mean} 24.280	2.0			C_{mean} 0.12		200		C_{mean} 0.76
	C_{trough} 4.27	2.5			C_{trough} 0.04				C_{trough} 0.19
5 BD	C_{max} 75.97	3.0		60 BD	C_{max} 0.52			40 OD	C_{max} 3.69
	C_{mean} 42.83	3.5			C_{mean} 0.31				C_{mean} 1.57
	C_{trough} 16.36	4.0			C_{trough} 0.12				C_{trough} 0.40
10 OD	C_{max} 121.97							30 BD	C_{max} 2.74
	C_{mean} 48.56								C_{mean} 1.95
	C_{trough} 8.54								C_{trough} 0.95
10 BD	C_{max} 151.9							105 OD (1.5 mg/kg)	C_{max} 12.8
	C_{mean} 85.66								C_{mean} 5.47
	C_{trough} 32.73								C_{trough} 1.40
20 OD	C_{max} 195.15							70 BD (1 mg/kg)	C_{max} 10.79
	C_{mean} 77.69								C_{mean} 7.67
	C_{trough} 13.66								C_{trough} 3.74
20 BD	C_{max} 243.10								
	C_{mean} 137.06								
	C_{trough} 52.37								
53 OD	C_{max} 387.86								
	C_{mean} 154.42								
	C_{trough} 27.15								
53 BD	C_{max} 483.17								
	C_{mean} 272.42								
	C_{trough} 104.08								

53 mg OD/BD doses (although not used in clinical studies) were simulated to double exposure (C_{mean}) of 20 mg OD/BD, taking into account the less than dose-proportional increase in exposure due to reduced absorption, observed at high doses [3,26]. A control without any drugs was also run in the model. BD, twice daily; C_{max}, maximum drug concentration; C_{mean}, average drug concentration; C_{trough}, minimum drug concentration; INR, international normalized ratio; IV, intravenous; OD, once daily; s.c., subcutaneous.

doi:10.1371/journal.pone.0017626.t001

region of experimentally obtained values in the model of Hockin et al. [10], was reduced in our model. The action of von Willebrand factor was introduced based on the scheme and rate constants published by Saenko et al. [24].

Drug action

All study drugs were modelled by a representation of their anticoagulant properties using what was known from published information. Values for direct kinetic constants (k_{on} and k_{off}) were used when available. When no direct experimental kinetic data for individual biochemical reactions were available, values were determined numerically by fitting the model behaviour to indirect measurements using PT and aPTT values versus drug concentrations. A broad set of regimens (doses and schedules) was simulated, both with constant drug levels and dynamic pharmacokinetic profiles (Table 1).

Rivaroxaban. Rivaroxaban acts via complexation to free Factor Xa and to the prothrombinase complex (Factor Xa and activated Factor V [Factor Va]; Table 2) [2]. Experimental kinetic data were available for the reaction of complexation to Factor Xa [25]. Kinetic constants were calculated and fitted into the model based on measured Ki values [2] and experimental PT–rivaroxaban plasma concentration relationships [26]. The binding of rivaroxaban to proteins was modelled as a complexation/decomplexation reaction (RBay3), and kinetic constants were calculated and fitted into the model based on the values of measured fraction of unbound drug and PT versus

Table 2. Modelling of drug action.

Reaction name	Stoichiometry	Kinetics
Rivaroxaban action		
RBay1	Bay59_7939+Xa→Bay59_7939_Xa	Bay59_7939*Xa*kBay1-Bay59_7939_Xa*kBay1*kBay_Ki_Xa
RBay1s	Bay59_7939+Xa_lipid→Bay59_7939_Xa_lipid	Bay59_7939*Xa_lipid*kBay1-Bay59_7939_Xa_lipid*kBay1*kBay_Ki_Xa
RBay2	Bay59_7939+Xa_Va_lipid→Bay59_7939_Xa_Va_lipid	Bay59_7939*Xa_Va_lipid*kBay3-Bay59_7939_Xa_Va_lipid*kBay3*kBay_Ki_XaVa
RBay3	Bay59_7939_Bound→Bay59_7939	kBay_fu_on*kBay_fu*Bay59_7939_Bound-kBay_fu_on*Albumin_Factor*Bay59_7939
RBay4	Bay59_7939_Xa+ATIII→Bay59_7939_Xa_ATIII	kBay5*Bay59_7939_Xa*ATIII
RBay5	Bay59_7939+Xa_ATIII→Bay59_7939_Xa_ATIII	kBay6*Bay59_7939*Xa_ATIII-kBay6*kBay_Ki_XaATIII*Bay59_7939_Xa_ATIII
DX-9065a action		
RDx1	DX9065a+Xa→DX9065a_Xa	kDx1*DX9065a*Xa-kDx2*DX9065a_Xa
RDx1s	DX9065a+Xa_lipid→DX9065a_Xa_lipid	kDx1*DX9065a*Xa_lipid-kDx2*DX9065a_Xa_lipid
RDx2	DX9065a+Xa_Va_lipid→DX9065a_Xa_Va_lipid	kDx3*DX9065a*Xa_Va_lipid-kDx4*DX9065a_Xa_Va_lipid
RDx3	DX9065a_Xa+ATIII→DX9065a_Xa_ATIII	kDx5*DX9065a_Xa*ATIII
RDx4	DX9065a→Dx9065a_Bound	kDx_fu_on*Albumin_Factor*Dx9065a-kDx_fu_on*kDx_fu*DX9065a_Bound
RDx5	DX9065a+Xa_ATIII→DX9065a_Xa_ATIII	kDx6*DX9065a*Xa_ATIII-kDx7*DX9065a_Xa_ATIII
(Xi)Melagatran action		
RXi1	Xim+IIa→IIa_Xim	kXim1*IIa*Xim-kXim2*IIa_Xim
RXi2	Xim+mIIa→mIIa_Xim	kXim3*mIIa*Xim-kXim4*mIIa_Xim
RXi3	Xim+IIa_Tm→IIa_Tm_Xim	kXim5*IIa_Tm*Xim-kXim6*IIa_Tm_Xim
RXi4	Xim→Xim_Bound	kXim_fu_on*Albumin_Factor*Xim-kXim_fu_on*kXim_fu*Xim_Bound
Enoxaparin action		
RHep1	Hep→Hep_Bound	kHep_fu_on*Albumin_Factor*Hep-kHep_fu_on*kHep_fu*Hep_Bound
RHep2	ATIII+Hep→ATIIIa	kHep_ATIII_on*ATIII*Hep-kHep_ATIII_on*kHep_Ki_ATIII*ATIIIa
RHep3	Xa+ATIIIa→Xa_ATIII+Hep	kHep_Xa_ATIIIa*Xa*ATIIIa
RHep4	Xa_lipid+ATIIIa→Xa_ATIII+PhosphoLipid+Hep	kHep_Xa_ATIIIa*Xa_lipid*ATIIIa
RHep5	Xa_Va_lipid+ATIIIa→Xa_ATIII+Hep+Va_lipid	kHep_XaVa_ATIIIa*Xa_Va_lipid*ATIIIa
RHep6	IIa+ATIIIa→IIa_ATIII+Hep	kHep_IIa_ATIIIa*IIa*ATIIIa
RHep7	mIIa+ATIIIa→mIIa_ATIII+Hep	kHep_IIa_ATIIIa*mIIa*ATIIIa
RHep8	ATIIIa+IXa→IXa_ATIII+Hep	kHep_IXa_ATIIIa*IXa*ATIIIa
RHep9	ATIIIa+IXa_lipid→IXa_ATIII+PhosphoLipid+Hep	kHep_IXa_ATIIIa*IXa_lipid*ATIIIa
RHep10	XIa+ATIIIa→XIa_ATIII+Hep	kHep_XIa_ATIIIa*XIa*ATIIIa
RHep11	XIa_lipid+ATIIIa→XIa_ATIII+PhosphoLipid+Hep	kHep_XIa_ATIIIa*XIa_lipid*ATIIIa

Va, IIa, IXa, Xa and XIa denote activated coagulation factors. ATIII, antithrombin; BAY59-7939, rivaroxaban; fu, fraction unbound; Hep, heparin (here parameterized as enoxaparin); on, k_{on}, association rate constant; mIIa, meizothrombin; Tm, thrombomodulin; Xim, ximelagatran active metabolite (melagatran).
doi:10.1371/journal.pone.0017626.t002

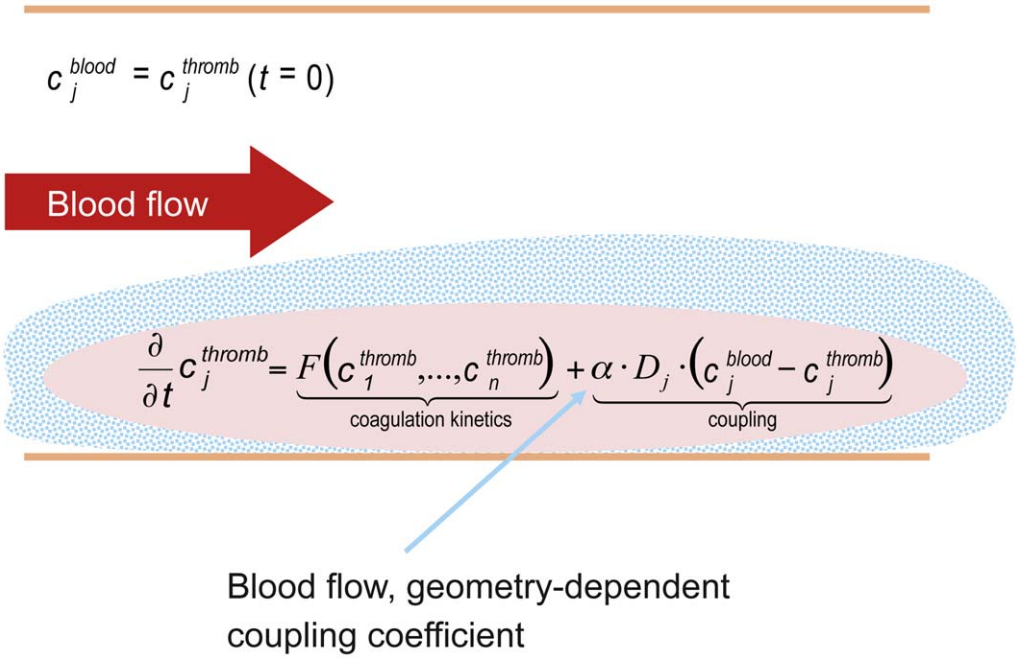

Figure 2. Modelling of blood flow. The top equation represents the initial condition where the concentration of each species c_j is the same for the coagulation zone 'thromb' and the reservoir 'blood'. The first element of the bottom equation ('coagulation kinetics') represents the coagulation processes (i.e. the biochemical kinetics of the model), whereas the second element ('coupling') represents the flowing conditions. α, general coupling constant, as a function of blood flow and geometry (size of vessels); c_j, concentration of coagulation factor; D_j, diffusion–convection coefficient; F, blood coagulation cascade model coefficient.
doi:10.1371/journal.pone.0017626.g002

rivaroxaban plasma concentration relationships. This method was used to model protein binding for all other study drugs, with some variations to take the different mechanisms of action into account.

DX-9065a. The method used to fit DX-9065a into the model was similar to that used for rivaroxaban, because the two drugs have a similar mechanism of action [27]. Because DX-9065a–Factor Xa complexes can bind Factor Va, this reaction was added to the model (RDx3; Table 2). All kinetic constants and the structure of the model (pharmacological values) were found in the literature [28–32].

Ximelagatran. The binding reactions of melagatran (the active metabolite of ximelagatran) to Factor IIa, meizothrombin (mIIa), and the thrombin–thrombomodulin complex were added into the model (RXi1 to RXi4; Table 2). All kinetic constants and the structure of the model (mechanistic mode of action) were found in the literature [33–38].

Enoxaparin. The complexation of enoxaparin to AT, and the subsequent reactions of this complex with Factor Xa, the Factor Xa–Factor Va complex (prothrombinase), Factor IIa, mIIa, Factor IXa and Factor XIa were added into the model (Table 2, RHep1 to RHep11). The major inhibitory effect is on Factor Xa (free and lipid bound), which is reflected by the highest rate constant. The model takes into account the dissociation of enoxaparin after any of these targets is bound to activated AT, and enoxaparin is released, allowing it to activate another molecule of AT.

Warfarin. The action of warfarin was not modelled explicitly, but represented by a shift in initial conditions (starting concentrations) for vitamin K-dependent Factors II, VII, IX and X, as well as proteins C and S based on published data [39]. To reach a given therapeutic international normalized ratio (INR), each vitamin K-dependent Factor concentration was simultaneously reduced to the required percentage of the normal value.

Table 3. *In vivo* coagulation scenarios included in the model.

Scenario	Tissue factor concentration (M)	Factor XIIa concentration (M)
Extrinsic strong	10^{-11}	0
Extrinsic weak	10^{-14}	0
Intrinsic strong	0	10^{-11}
Intrinsic weak	0	10^{-14}

doi:10.1371/journal.pone.0017626.t003

Blood flow

The model had to take into account the fact that in vivo coagulation is not only triggered by weak TF and Factor XIIa concentrations and propagated by the coagulation cascade, but is also affected by blood flow and the resulting exchange of proteins between the clotting region (and its surrounding area, named 'thromb') and the fresh blood pool that generally includes non-activated coagulation factors (Figure 2). The model described so far was coupled with an infinite pool of plasma (named 'blood') to represent the loss of activated factors and the supply of non-activated factors due to blood flow and diffusion (Figure 2). We used an approach similar to Kuharsky and Fogelson [13] and assumed a linear flow parameter, which was identical for all transported species, to describe the mass exchange. This resulted in transport reactions for each species X in the model (see: Appendix S1 and Appendix S2) of the form:

$$\alpha \times \mathrm{D} \times (\mathrm{X\_blood} - \mathrm{X\_thromb})$$

The only species not transported are those bound to immobile tissue or to the thrombus (i.e. TF and all its formed complexes with

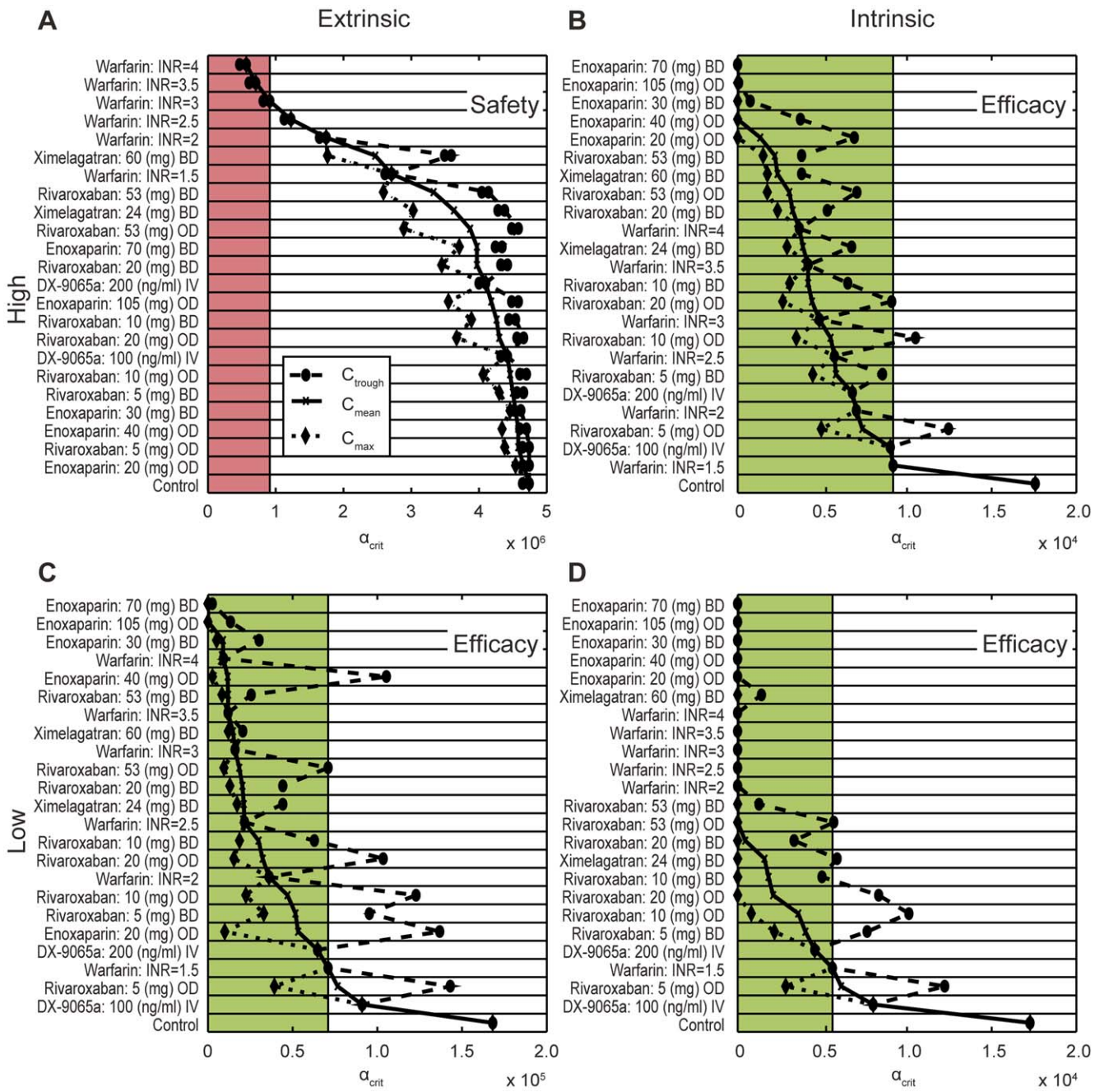

Figure 3. Benchmarking of anticoagulants based on thresholds for blood flow-mediated washout using physiologically plausible trigger concentrations. The dashed line and dots and the dotted line and the diamonds indicate the spread of the threshold for blood flow- and diffusion-mediated washout of a clot formation (α_{crit}, seconds; Methods) within the therapeutic concentration range (difference between C_{trough} and C_{max}); α_{crit} at C_{mean} is indicated by the solid line and crosses. The strong extrinsic trigger (TF 10^{-11} mol/l, seconds; Table 3) is considered as safety relevant (A). The (red) shaded area indicates safety-relevant prolongation of clotting times above the effect of warfarin titrated to an INR of 3, which is used as a safety reference. All therapies above the level of this therapy are considered safe. The other three triggers (B: Factor XIIa 10^{-11} mol/l; C: TF 10^{-14} mol/l; D: 10^{-14} mol/l) are considered as efficacy relevant. The effect of warfarin titrated to an INR of 1.5 is used as an efficacy reference and all therapies reaching inhibition above the level of this therapy, i.e. α_{crit} values below the reference level (green shaded area) are considered efficacious. BD, twice daily; C_{max}, maximum concentration; C_{mean}, mean concentration; C_{trough}, minimum concentration; INR, international normalized ratio; IV, intravenous; OD, once daily; TF, tissue factor.
doi:10.1371/journal.pone.0017626.g003

other species and the fibrin cleavage product Ia). Coupling was determined by a general coupling constant (α), which controls the overall strength of the coupling, and a Factor-dependent diffusion–convection constant, termed D (set to 5×10^{-7} cm^2/s, averaged from the more complex hydrodynamic approach of Anand et al. (Table 3) [14]. When α is zero, the flow model is equal to the static model; increasing α represents an increase of the blood flow. The lowest exchange rate (i.e. the critical value of α [α_{crit}]), which suppresses a coagulation event for a given trigger scenario, was calculated, and comparisons of the different α_{crit} values for the

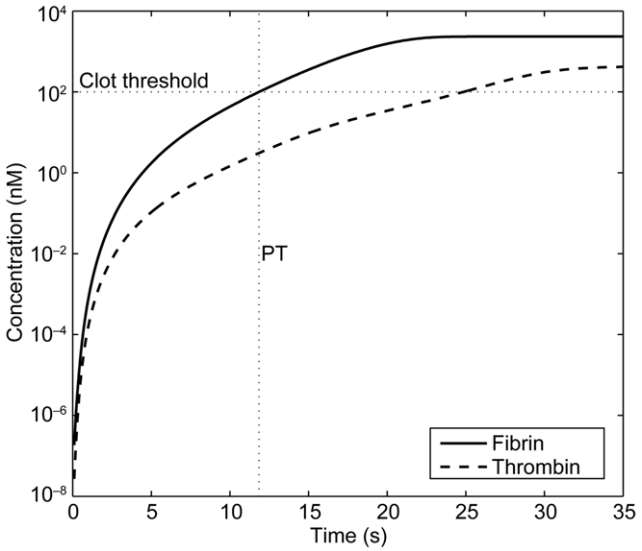

Figure 4. Implementation of PT into *in vitro* coagulation scenarios. Simulation of a PT scenario, thrombin and fibrin generation. PT, prothrombin time.
doi:10.1371/journal.pone.0017626.g004

study drugs were a useful model output to benchmark compounds and dosing schedules (Results, Figure 3). However, there were no means to determine α_{crit} directly or correlate it to an experimentally accessible value. Furthermore, it is important to note that this model only focused on the onset of coagulation (i.e. that fibrinolysis was not included in this model).

Initial conditions

The initial concentrations for all modelled coagulation factors and other proteins are given in Appendix S2. Depending on the coagulation scenario (*in vitro* or *in vivo*), individual factors not listed in Appendix S2, such as TF or Factor XIIa/Factor XIa (i.e. the triggers), were set to values other than zero, as for the values given in Table 3 or described below for PT and aPTT.

Kinetic parameters

Kinetic parameters, including kinetic and diffusion constants, are given in Appendix S3. These constants are independent of the simulated coagulation scenario, except for the general flow coupling constant α, the dilution factor (see below), and the albumin–factor coupling constant, which describes the dilution of albumin and affects the unbound fraction of the different study drugs.

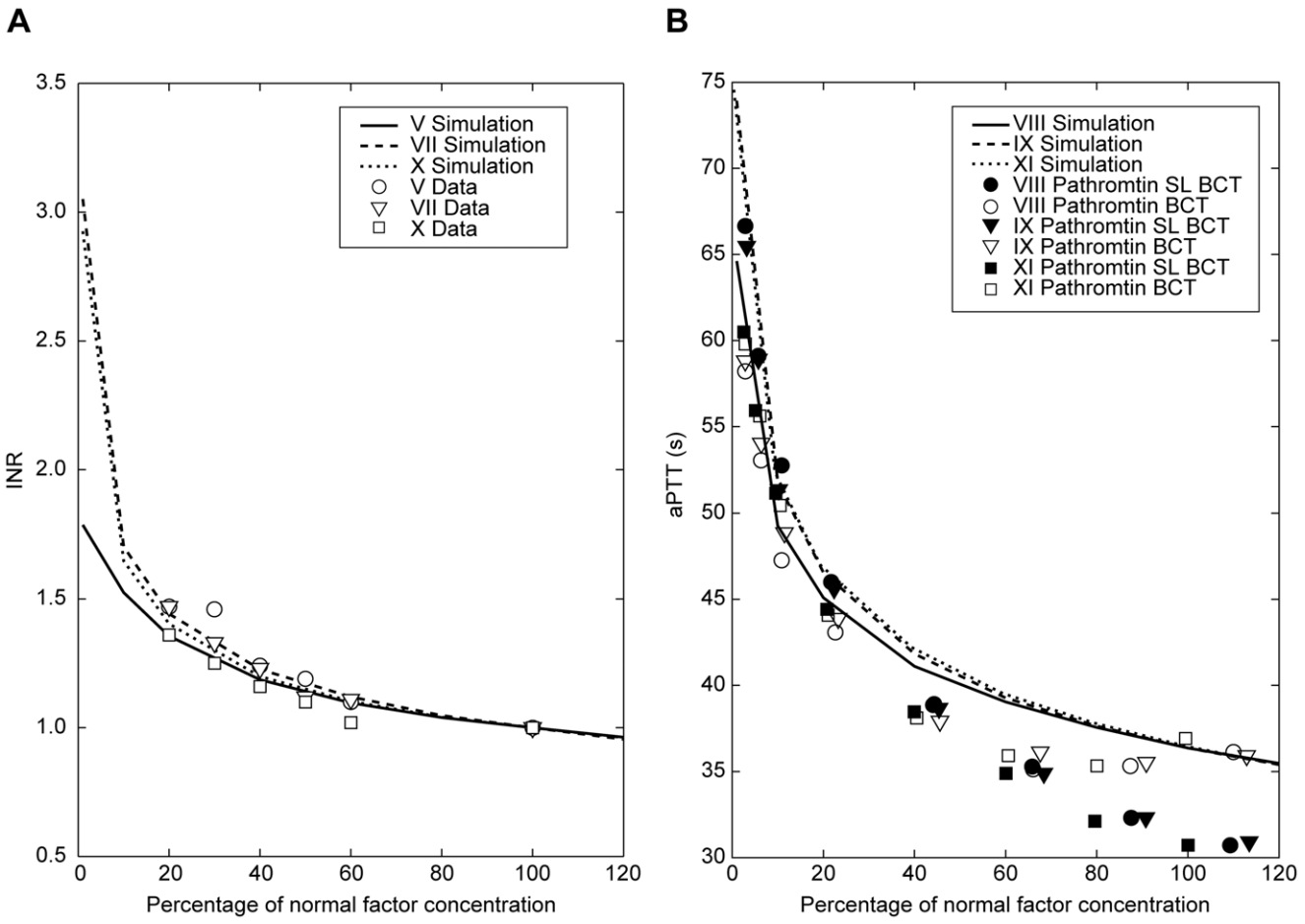

Figure 5. Simulation of coagulation factor variations and comparison with published experimental data. (A) published PT INR data from Fisher Diagnostics 1999 [40] and with (B) published aPTT data from Kappert 2002 [41]. Reagents used in aPTT reference studies: Pathromtin® SL (SL; Behringwerke AG, Marburg, Germany) and Behring Coagulation Time (BCT). aPTT, activated partial thromboplastin time; INR, international normalized ratio; PT, prothrombin time.
doi:10.1371/journal.pone.0017626.g005

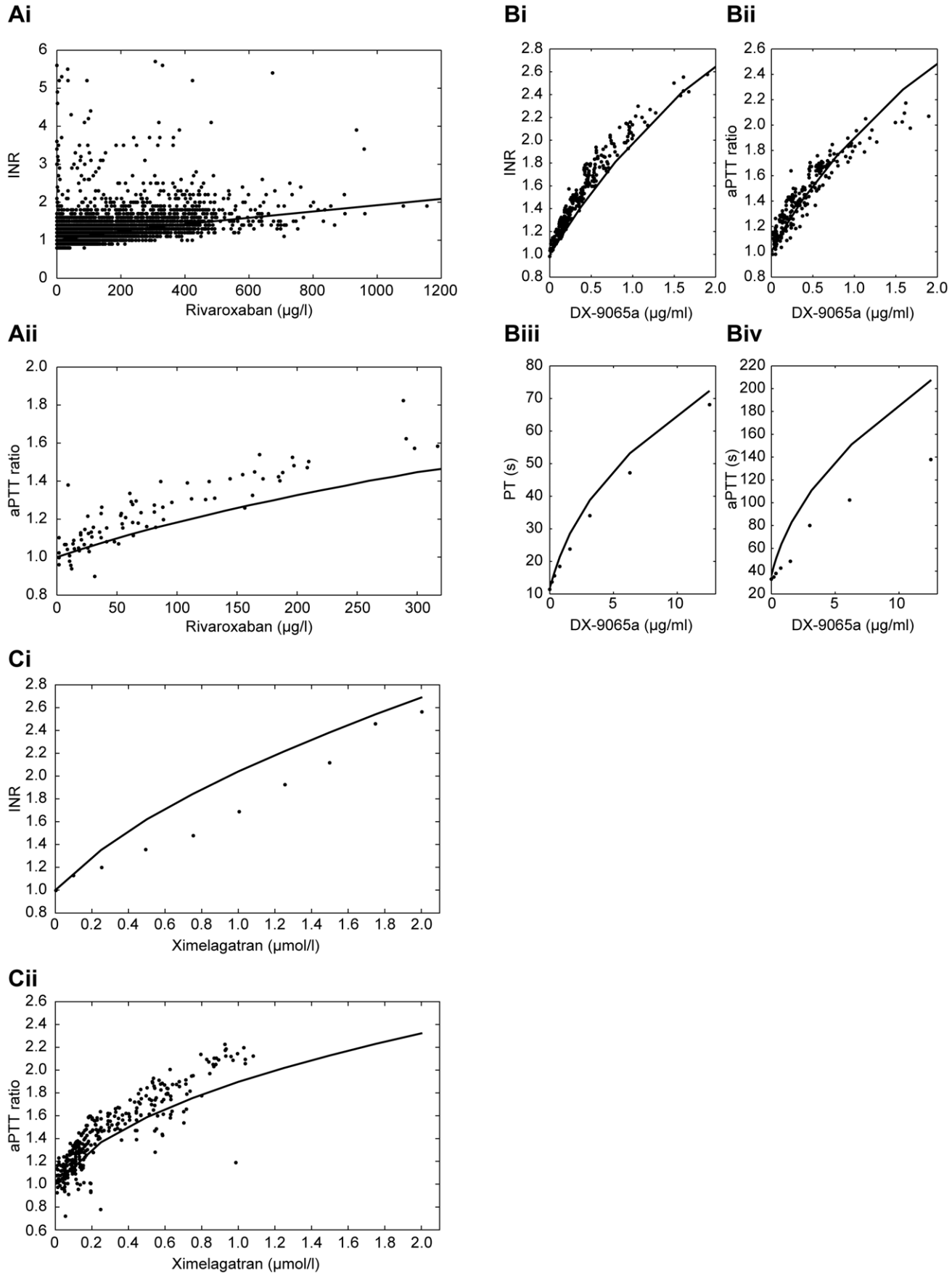
Ai
INR
Rivaroxaban (μg/l)
Aii
aPTT ratio
Rivaroxaban (μg/l)
Bi
INR
DX-9065a (μg/ml)
Bii
aPTT ratio
DX-9065a (μg/ml)
Biii
PT (s)
DX-9065a (μg/ml)
Biv
aPTT (s)
DX-9065a (μg/ml)
Ci
INR
Ximelagatran (μmol/l)
Cii
aPTT ratio
Ximelagatran (μmol/l)

Figure 6. PT and aPTT dependent on plasma concentration of anticoagulant drugs. (A) rivaroxaban (experimental data from internal studies); (B) DX-9065a (experimental data from the literature [30,31,41]; and (C) ximelagatran (experimental data for PT and aPTT from the literature [36,37]. aPTT, activated partial thromboplastin time; INR, international normalized ratio; PT, prothrombin time.
doi:10.1371/journal.pone.0017626.g006

Implementation of coagulation scenarios – *in vitro* scenarios

Dilution of plasma by a coagulation reagent was defined as reduced concentrations of all plasma proteins and factors, as well as added drugs, or as adjusted effective concentrations for surface-bound factors (e.g. TF). Initial plasma concentrations of inhibitors (study drugs) were calculated based on pharmacokinetic data.

Prothrombin time. All concentrations given in Appendix S2 were reduced to a factor of one-third to account for *in vitro* dilution, in order to reproduce the procedures generally used for the PT test. The tests require that an aliquot of plasma be mixed with an aliquot of coagulation test reagent containing trigger(s), phospholipids, calcium ions and buffer. To initiate a PT test, TF 4 nM concentrations were used, together with preactivated 1% of Factor V taken from [10]. PT was defined as the time when the fibrin concentration reached 100 nM for the first time (Figure 4), meaning that after dilution in the assay, more than 4% of the physiological amount of fibrinogen (7 µM, see Appendix S2) had been activated for clot formation. This was found to be the starting point of a massive cleavage of fibrinogen in the model. The INR was calculated by simply dividing PT with study drug by PT without study drug, thus assuming an ISI exponent of 1 for our simulated PT reagent. The dependence of the INR on individual coagulation factor variance was simulated and compared with published data [40]. The quality of the fit (Figure 5A) was used as validation for the model.

Activated partial thromboplastin time. All concentrations given in Appendix S2 were reduced to a factor of one-third to account for *in vitro* dilution and to reproduce the procedures generally used for the aPTT test. To initiate an aPTT test, 2.2 nM Factor XIa and 50 nM Factor XIIa concentrations were used, together with preactivated 1% of Factor V taken from [10]. The coagulation factor variations were simulated and compared with published data [40,41]. The quality of the fit (Figure 5B) was used as validation for the model.

Implementation of coagulation scenarios – *in vivo* scenarios

To mimic *in vivo* conditions relevant to bleeding risks under anticoagulant therapy and relevant to thrombosis, four trigger scenarios were constructed (Table 3). All four scenarios are considered to be more closely related to physiological conditions than classical *ex vivo* laboratory tests, where trigger concentrations many orders of magnitude higher than those occurring *in vivo* have to be used for practical reasons.

As a safety-relevant strong trigger, a high TF concentration (10^{-11} mol/l) representing contact with subendothelial tissue was chosen. Prolongation of clotting times under this scenario was interpreted as an increased bleeding risk. To investigate efficacy, three triggers (a low TF concentration, 10^{-14} mol/l, and two Factor XIIa concentrations, 10^{-11} and 10^{-14} mol/l) were separately applied, which represent typical situations where massive clotting should not occur, simulating plasma not in contact with subendothelial tissue. In such scenarios, a significant clotting would raise the risk of thrombosis. These three triggers are interpreted as a complement to the bleeding scenario.

Besides the direct calculation of clotting times under all four trigger scenarios, α_{crit} values were also determined for all these scenarios with and without anticoagulants, the results being used for benchmarking of therapies.

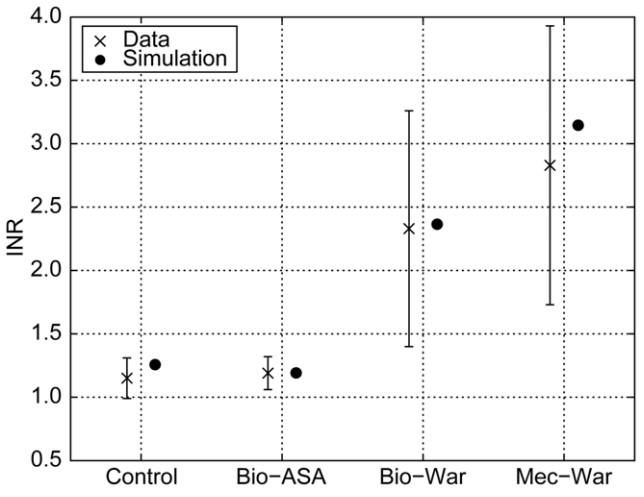

Figure 7. Comparison of simulated with measured INR values. One control group (Control) without medication and three patient groups: mechanical (Mec) or biological (Bio) heart valve replacement with different co-medications (acetylsalicylic acid [ASA] or warfarin [War]) at different target INRs with model predictions of INRs [47]. Simulated INR values were based on measurements of the mean concentrations of Factors II, VII, X, protein C and protein S resulting from therapy. Factor IX was set to the average concentration of the measured factors. INR, international normalized ratio.
doi:10.1371/journal.pone.0017626.g007

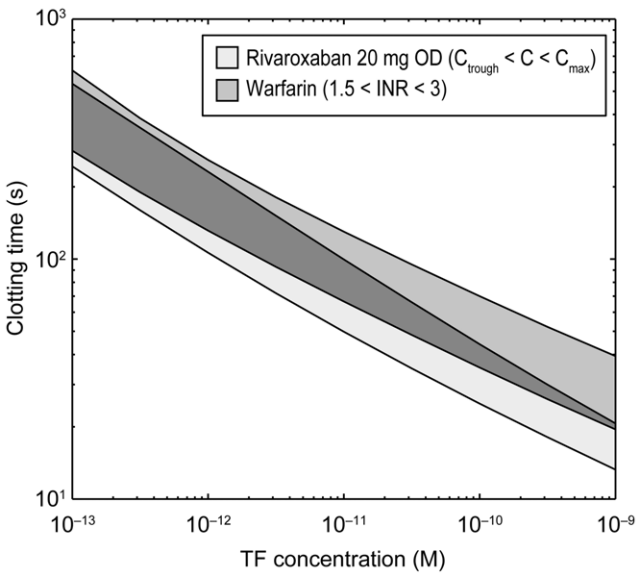

Figure 8. Simulation of thrombus inhibition with rivaroxaban and warfarin. Rivaroxaban concentrations at 20 mg once daily: C_{max} 251 ng/ml, C_{trough} 30 ng/ml. The width of the rivaroxaban curve reflects the C_{trough} to C_{max} concentration range and the width of the warfarin curve reflects the typically used INR range. C_{max}, maximum concentration; C_{trough}, minimum concentration; INR, international normalized ratio; OD, once daily; TF, tissue factor.
doi:10.1371/journal.pone.0017626.g008

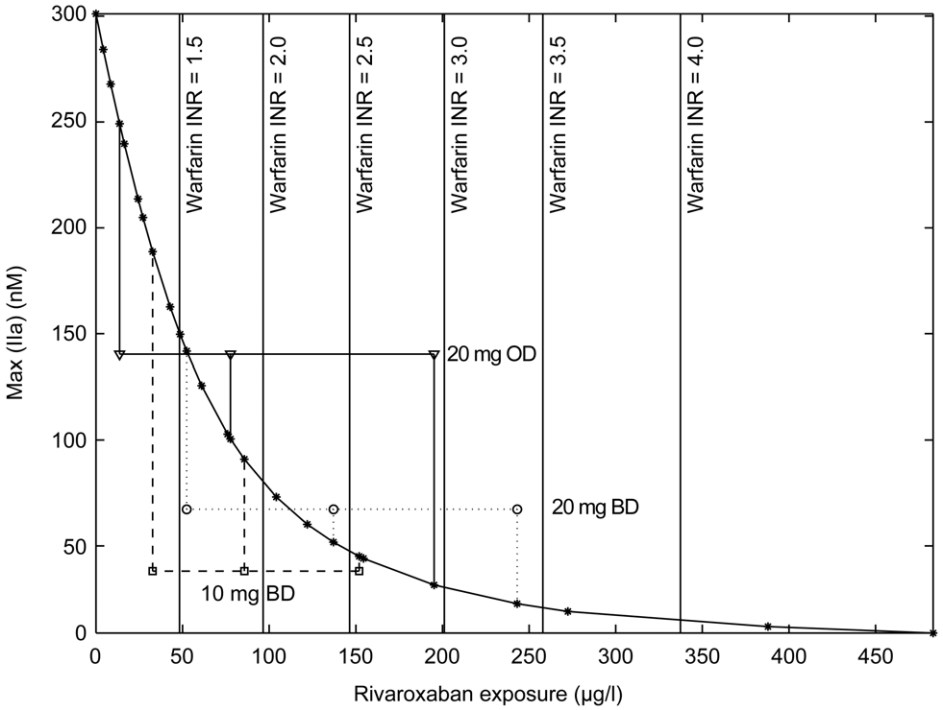

Figure 9. Effect of rivaroxaban exposure on thrombin peak height. This graph shows the effect of increasing concentration of rivaroxaban on thrombin peak height for a 5×10^{-12} mol/l tissue factor trigger (dilution 2:3, 4 µM phospholipid, corresponding to an *in silico* thrombin generation assay). To compare this with warfarin therapy, the corresponding values for INRs (1.5–4.0) are marked by vertical lines. The ranges for C_{max}, C_{mean} and C_{trough} reflect experimental rivaroxaban values found in dose-finding studies [48,50,55]. The simulated thrombin peak reduction is in the range of therapeutically used INRs. BD, twice daily; C_{max}, maximum concentration; C_{mean}, mean concentration; C_{trough}, minimum concentration; INR, international normalized ratio; OD, once daily.
doi:10.1371/journal.pone.0017626.g009

Results

Drug action mechanism models of rivaroxaban and other anticoagulants

Comparisons were made between experimental concentration–response profiles (data taken from the literature [30,31,36,37,42] or from in-house studies conducted with rivaroxaban) and simulation results for all study drugs. Plots for PT and aPTT that are dependent on plasma concentrations of rivaroxaban, DX-9065a and ximelagatran in Figures 6A, 6B and 6C, respectively, compare the experimental data with simulated plots for these three drugs [30,31,36,37,42].

Enoxaparin concentrations in blood are determined in anti-Factor Xa units because it is not a homogenous substance but a mixture of different oligomers [38]. However, using the reported value of 100 units per mg enoxaparin and an average molecular weight of 4500 g/mol, approximate molar concentrations required for modelling can be obtained. PT and aPTT values as a function of plasma concentrations are reported to be not meaningful within the therapeutic concentration range [38], thus being less suited for a model calibration. Anti-Factor Xa values alone on the other hand are not sufficient to validate inactivation kinetics. However, several publications reporting kinetic constants are available [27,43–45]. Averages of these published *in vitro* values were used in our model (Appendix S3, parameters starting with kHep). Simulated PT and aPTT values increased only marginally within therapeutic concentrations (data not shown).

Typical subcutaneous doses are between 20 mg once daily (od) and 30 mg twice daily (bid) for prevention, and 1.5 mg/kg od or 1.0 mg/kg bid for acute therapy. We obtained corresponding plasma concentrations from the manufacturer's data sheets [38] and from the public files of the registration agencies [46]. Unavailable concentrations were taken or extrapolated from in-house measured enoxaparin pharmacokinetic curves. Table 1 lists the concentrations used in our simulations.

Warfarin validation results are shown in Figure 7. The resulting prolongations of the simulated PT values, depicted as INRs, were in good agreement with published data [47]. Variations in experimental data were primarily caused by individual variations in factor concentrations, which are frequent with warfarin therapy, and less by experimental error. Simulations were conducted for the mean concentrations and, therefore, the results presented are close to the actual mean INR data.

Applications of the model to clinical studies

Efficacy and safety compared with warfarin. Rivaroxaban 20 mg od was compared with warfarin (INR 1.5–3.0). Clotting times were measured as a function of TF concentrations (Figure 8). At low TF concentrations, the therapeutic INR window for warfarin has a large overlap with the concentration window of the direct Factor Xa inhibitor. By contrast, warfarin shows a stronger effect (i.e. prolongation) on clotting times at higher TF concentrations than the direct Factor Xa inhibitor rivaroxaban. In other words, the mechanism of direct Factor Xa inhibition shows a steeper dependency on TF trigger concentrations than vitamin K-dependent inhibition of the coagulation systems. There is a clear tendency to higher potency at low (i.e. thrombosis relevant) TF concentrations and a lower potency at high TF concentrations where anticoagulant effects could lead to bleeding.

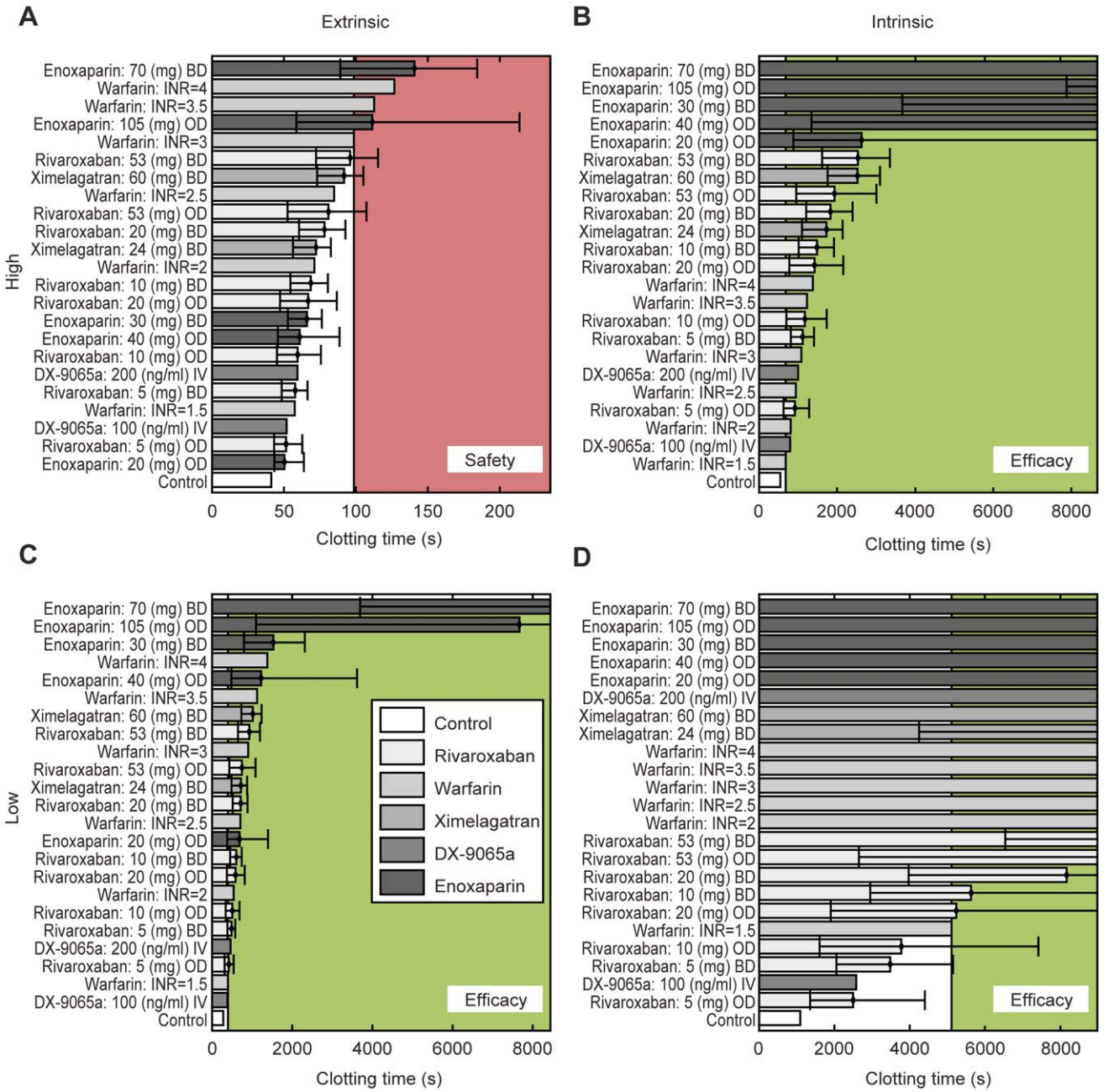

Figure 10. Benchmarking of anticoagulants based on clotting times using physiologically plausible trigger concentrations. Error bars show the spread of the clotting time within the therapeutic concentration range (difference between C_{trough} and C_{max}); clotting time at C_{mean} was used for the main bar. The strong extrinsic trigger (TF 10^{-11} mol/l, seconds; Table 3) is considered as safety relevant (A). The (red) shaded area indicates safety-relevant prolongation of clotting times above the effect of warfarin titrated to an INR of 3, which is used as a safety reference. All therapies below the level of this therapy are considered safe. The other three triggers (B: Factor XIIa 10^{-11} mol/l; C: TF 10^{-14} mol/l; D: 10^{-14} mol/l) are considered as efficacy relevant. The effect of warfarin titrated to an INR of 1.5 is used as an efficacy reference and all therapies reaching inhibition above the level of this therapy (green shaded area) are considered efficacious. BD, twice daily; C_{max}, maximum concentration; C_{mean}, mean concentration; C_{trough}, minimum concentration; INR, international normalized ratio; i.v., intravenous; OD, once daily, TF, tissue factor.
doi:10.1371/journal.pone.0017626.g010

Plasma concentrations of a direct Factor Xa inhibitor required to achieve effects similar to warfarin therapy, titrated to different INR values, were then calculated. Figure 9 shows peak concentrations of Factor IIa obtained for a trigger scenario with 5×10^{-12} mol/l TF, (between the value of the extrinsic strong and weak triggers of Table 3), and increasing rivaroxaban concentrations. The concentration–effect curve shows a steep slope at low rivaroxaban concentrations and levels off at concentrations above 150 μg/l. According to this simulated scenario, this type of concentration–effect relationship appears optimal for a broad therapeutic window. Both the under-dosing and over-dosing risks are minimized because low concentrations in the order of the C_{trough} concentrations of Table 1 already reach significant efficacy levels, and variance at high concentrations result in minimal reduction of the thrombin peak.

Dose-finding studies. The therapeutic window of rivaroxaban was estimated by comparing rivaroxaban with ximelagatran,

enoxaparin, DX-9065a and warfarin. The study drugs were simulated and ranked for their effect on clotting time and α_{crit} with all triggers from the panel of physiologically plausible intrinsic and extrinsic activations (Methods, Table 3). Typical doses for all drugs were obtained after reviewing the literature. Figure 10 shows the ranking of clotting times for all scenarios tested. For safety assessment, the warfarin effect at an INR of 3 was used as a reference (upper threshold, red shaded area). For efficacy assessment, the warfarin effect at an INR of 1.5 was used (lower threshold, green shaded area). Using this (relative) measure, all rivaroxaban therapies up to a dose of 20 mg bid are considered safe. Depending on the efficacy scenario, daily doses of rivaroxaban above 5 mg appear to be efficacious, with a daily dose of 20 mg reaching the efficacy window in all three scenarios. Similar results were obtained with the calculation of the α_{crit} levels; daily doses of rivaroxaban between 5 mg and 40 mg appear to be safe and efficacious, with a possible optimal dose of approximately 20 mg per day.

Discussion

The blood coagulation modelling presented in this paper allows robust simulation of clinically relevant blood coagulation tests and of *in silico* experiments that simulate flowing blood. The effects of coagulation inhibitors acting upon coagulation factors can be easily simulated using the graphical user interface MoBi. In combination with experimental or simulated pharmacokinetic data, therapeutic ranges for the drugs included in the model can be evaluated and efficacy and safety limits can be determined.

The comparative analysis of the mechanism of direct Factor Xa inhibition (rivaroxaban) showed a dependency on TF trigger strength favourable to the vitamin K-dependent inhibition of the coagulation system (Figure 8). At low trigger concentrations assumed to be relevant for thrombosis prevention, the potency of both mechanisms of action is similar, but at high trigger concentrations, relevant for bleeding risk assessment, the effect of direct inhibition is smaller. The concentration–effect curve of rivaroxaban (Figure 9) shows a pronounced convex shape. The increase of inhibition at low inhibitor concentrations is much steeper than at high concentrations. Together with the TF concentration dependency, this result supports the assumption of a broad therapeutic range for direct Factor Xa inhibition.

The therapeutic window for rivaroxaban found by simulating and ranking a broad portfolio of anticoagulants and scenarios was a total daily dose between 5 mg and 40 mg (Figures 3 and 10). Within this window, direct Factor Xa inhibition with rivaroxaban compares well with other currently used or developed anticoagulant therapies and consistently outperforms vitamin K-dependent inhibition (warfarin). A 20 mg od dose yielded favourable coagulation results, i.e. the safety margin of an INR 3 warfarin therapy was not exceeded, and efficacy was better than an INR 1.5 therapy (see Figures 3 and 10). Dose-finding, phase IIb studies of rivaroxaban for the prevention of venous thromboembolism in patients undergoing total hip and knee replacement showed that 5–20 mg total daily doses had efficacy and safety similar to that of enoxaparin, thereby demonstrating a wide therapeutic window for rivaroxaban [48,49].

After another phase II study investigating the once-daily dosing of rivaroxaban in patients undergoing total hip replacement [50], the 10 mg od dose was considered to provide the optimal balance between efficacy and safety. It was selected for further development in the phase III RECORD programme, which investigated the prevention of venous thromboembolism after total hip or total knee replacement [51–54].

After two dose-ranging phase II studies for the treatment of venous thromboembolism [55,56], a starting dose of 15 mg bid followed by a 20 mg od maintenance dose of rivaroxaban was selected for phase III studies in this indication. These doses are within the therapeutic window of 5–50 mg determined by the present computer model, thereby confirming its usefulness and quantitative accuracy. Potential applications in modelling include other aspects of coagulation, such as medication switch or the combination of antithrombotic therapies (e.g. anticoagulant plus platelet inhibitors) in the therapy of acute coronary syndrome.

Supporting Information

Appendix S1 Comprehensive reaction list of the coagulation model.
(DOC)

Appendix S2 Initial conditions for all species not being zero (coagulation factors and intrinsic inhibitors).
(DOC)

Appendix S3 Kinetic parameters for the model (based on mol/l and seconds).
(DOC)

Acknowledgments

The authors would like to acknowledge Chandrabala Shah who provided medical writing services with funding from Bayer Schering Pharma AG and Johnson & Johnson Pharmaceutical Research & Development.

Author Contributions

Conceived and designed the experiments: RB KC LK AS H-US JL WW TG. Performed the experiments: RB KC LK AS H-US JL. Analyzed the data: WM. Contributed reagents/materials/analysis tools: RB KC LK AS H-US JL TG WW. Wrote the paper: RB KC LK AS H-US JL WW TG WM.

References

1. Mann KG, Butenas S, Brummel K (2003) The dynamics of thrombin formation. Arterioscler Thromb Vasc Biol 23: 17–25.
2. Perzborn E, Strassburger J, Wilmen A, Pohlmann J, Roehrig S, et al. (2005) *In vitro* and *in vivo* studies of the novel antithrombotic agent BAY 59-7939 – an oral, direct Factor Xa inhibitor. J Thromb Haemost 3: 514–521.
3. Kubitza D, Becka M, Voith B, Zuehlsdorf M, Wensing G (2005) Safety, pharmacodynamics, and pharmacokinetics of single doses of BAY 59-7939, an oral, direct factor Xa inhibitor. Clin Pharmacol Ther 78: 412–421.
4. Ansell J, Hirsh J, Hylek E, Jacobson A, Crowther M, et al. (2008) Pharmacology and management of the vitamin K antagonists: American College of Chest Physicians evidence-based clinical practice guidelines (8th Edition). Chest 133: 160S–198S.
5. Hirsh J, Bauer KA, Donati MB, Gould M, Samama MM, et al. (2008) Parenteral anticoagulants: American College of Chest Physicians evidence-based clinical practice guidelines (8th Edition). Chest 133: 141S–159S.
6. Kubitza D, Haas S (2006) Novel factor Xa inhibitors for prevention and treatment of thromboembolic diseases. Expert Opin Investig Drugs 15: 843–855.
7. Mattsson C, Sarich TC, Carlsson SC (2005) Mechanism of action of the oral direct thrombin inhibitor ximelagatran. Semin Vasc Med 5: 235–244.
8. Stangier J, Clemens A (2009) Pharmacology, pharmacokinetics, and pharmacodynamics of dabigatran etexilate, an oral direct thrombin inhibitor. Clin Appl Thromb Hemost 15 Suppl 1: 9S–16S.
9. Bungay SD, Gentry PA, Gentry RD (2003) A mathematical model of lipid-mediated thrombin generation. Math Med Biol 20: 105–129.
10. Hockin MF, Jones KC, Everse SJ, Mann KG (2002) A model for the stoichiometric regulation of blood coagulation. J Biol Chem 277: 18322–18333.
11. Kogan AE, Kardakov DV, Khanin MA (2001) Analysis of the activated partial thromboplastin time test using mathematical modeling. Thromb Res 101: 299–310.
12. Orfeo T, Mann KG (2005) Mathematical and biological models of blood coagulation. J Thromb Haemost 3: 2397–2398.

13. Kuharsky AL, Fogelson AL (2001) Surface-mediated control of blood coagulation: the role of binding site densities and platelet deposition. Biophys J 80: 1050–1074.
14. Anand M, Rajagopal K, Rajagopal KR (2003) A model incorporating some of the mechanical and biochemical factors underlying clot formation and dissolution in flowing blood. J Theor Med 5: 183–218.
15. Bayer Technology Services (2009) MoBi®. Available: http://www.systems-biology.com/mobi. Accessed 18 Oct 2010.
16. Stevens WK, Cote HF, MacGillivray RT, Nesheim ME (1996) Calcium ion modulation of meizothrombin autolysis at Arg55-Asp56 and catalytic activity. J Biol Chem 271: 8062–8067.
17. Gilbert GE, Furie BC, Furie B (1990) Binding of human factor VIII to phospholipid vesicles. J Biol Chem 265: 815–822.
18. Ellis V, Scully M, MacGregor I, Kakkar V (1982) Inhibition of human factor Xa by various plasma protease inhibitors. Biochim Biophys Acta 701: 24–31.
19. Elisen MG, dem Borne PA, Bouma BN, Meijers JC (1998) Protein C inhibitor acts as a procoagulant by inhibiting the thrombomodulin-induced activation of protein C in human plasma. Blood 91: 1542–1547.
20. Heeb MJ, Gruber A, Griffin JH (1991) Identification of divalent metal ion-dependent inhibition of activated protein C by alpha 2-macroglobulin and alpha 2-antiplasmin in blood and comparisons to inhibition of factor Xa, thrombin, and plasmin. J Biol Chem 266: 17606–17612.
21. Hermans JM, Stone SR (1993) Interaction of activated protein C with serpins. Biochem J 295(Pt 1): 239–245.
22. van der Meer FJ, van Tilburg NH, van Wijngaarden A, van der Linden I, Briët E, et al. (1989) A second plasma inhibitor of activated protein C: alpha 1-antitrypsin. Thromb Haemost 62: 756–762.
23. Suzuki K, Nishioka J, Kusumoto H, Hashimoto S (1984) Mechanism of inhibition of activated protein C by protein C inhibitor. J Biochem 95: 187–195.
24. Saenko EL, Shima M, Sarafanov AG (1999) Role of activation of the coagulation factor VIII in interaction with vWf, phospholipid, and functioning within the factor Xase complex. Trends Cardiovasc Med 9: 185–192.
25. Perzborn E, Roehrig S, Straub A, Kubitza D, Mueck W, et al. (2010) Rivaroxaban: a new oral factor Xa inhibitor. Arterioscler Thromb Vasc Biol 30: 376–381.
26. Mueck W, Eriksson BI, Bauer KA, Borris L, Dahl OE, et al. (2008) Population pharmacokinetics and pharmacodynamics of rivaroxaban - an oral, direct factor Xa inhibitor - in patients undergoing major orthopaedic surgery. Clin Pharmacokinet 47: 203–216.
27. Rezaie AR (2003) DX-9065a inhibition of factor Xa and the prothrombinase complex: mechanism of inhibition and comparison with therapeutic heparins. Thromb Haemost 89: 112–121.
28. Alexander JH, Yang H, Becker RC, Kodama K, Goodman S, et al. (2005) First experience with direct, selective factor Xa inhibition in patients with non-ST-elevation acute coronary syndromes: results of the XaNADU-ACS Trial. J Thromb Haemost 3: 439–447.
29. Hara T, Yokoyama A, Ishihara H, Yokoyama Y, Nagahara T, et al. (1994) DX-9065a, a new synthetic, potent anticoagulant and selective inhibitor for factor Xa. Thromb Haemost 71: 314–319.
30. Ieko M, Tarumi T, Takeda M, Naito S, Nakabayashi T, et al. (2004) Synthetic selective inhibitors of coagulation Factor Xa strongly inhibit thrombin generation without affecting initial thrombin forming time necessary for platelet activation in hemostasis. J Thromb Haemost 2: 612–618.
31. Murayama N, Tanaka M, Kunitada S, Yamada H, Inoue T, et al. (1999) Tolerability, pharmacokinetics, and pharmacodynamics of DX-9065a, a new synthetic potent anticoagulant and specific factor Xa inhibitor, in healthy male volunteers. Clin Pharmacol Ther 66: 258–264.
32. Nagashima H (2002) Studies on the different modes of action of the anticoagulant protease inhibitors DX-9065a and Argatroban. I. Effects on thrombin generation. J Biol Chem 277: 50439–50444.
33. Adams TE, Everse SJ, Mann KG (2003) Predicting the pharmacology of thrombin inhibitors. J Thromb Haemost 1: 1024–1027.
34. Gustafsson D, Elg M (2003) The pharmacodynamics and pharmacokinetics of the oral direct thrombin inhibitor ximelagatran and its active metabolite melagatran: a mini-review. Thromb Res 109 Suppl 1: S9–S15.
35. Cullberg M, Eriksson UG, Wåhlander K, Eriksson H, Schulman S, et al. (2005) Pharmacokinetics of ximelagatran and relationship to clinical response in acute deep vein thrombosis. Clin Pharmacol Ther 77: 279–290.
36. Mattsson C, Menschiek-Lundin A, Wåhlander K, Lindahl TL (2001) Effect of melagatran on prothrombin time assays depends on the sensitivity of the thromboplastin and the final dilution of the plasma sample. Thromb Haemost 86: 611–615.
37. Eriksson UG, Bredberg U, Gislen K, Johansson LC, Frison L, et al. (2003) Pharmacokinetics and pharmacodynamics of ximelagatran, a novel oral direct thrombin inhibitor, in young healthy male subjects. Eur J Clin Pharmacol 59: 35–43.
38. Sanofi-Aventis (2009) Lovenox (enoxaparin sodium) Prescribing Information. Available: http://products.sanofi-aventis.us/lovenox/lovenox.pdf. Accessed 19 Oct 2010.
39. Wittkowsky AK (2003) Warfarin and other coumarin derivatives: pharmacokinetics, pharmacodynamics, and drug interactions. Semin Vasc Med 3: 221–230.
40. Fisher Diagnostics (1999) Thromboplastin correlation study. Available: http://web.archive.org/web/20070707124958/http://www.fisherdiagnostics.com/content/casestudies/thrombo7.pdf. Accessed 20 Oct 2010.
41. Kappert G (2002) Vergleichbarkeit der Methoden zur Bestimmung der Aktivierten Partiellen Thromboplastinzeit und der Resistenz gegen aktivertes Protein C. Available: http://docserv.uni-duesseldorf.de/servlets/DocumentServlet?id = 2417. Accessed 20 Oct 2010.
42. Tobu M, Iqbal O, Ma Q, Schultz C, Jeske W, et al. (2003) Global anticoagulant effects of a synthetic anti-factor Xa inhibitor (DX-9065a): implications for interventional use. Clin Appl Thromb Hemost 9: 1–17.
43. Mauray S, de Raucourt E, Talbot JC, Dachary-Prigent J, Jozefowicz M, et al. (1998) Mechanism of factor IXa inhibition by antithrombin in the presence of unfractionated and low molecular weight heparins and fucoidan. Biochim Biophys Acta 1387: 184–194.
44. Beguin S, Choay J, Hemker HC (1989) The action of a synthetic pentasaccharide on thrombin generation in whole plasma. Thromb Haemost 61: 397–401.
45. Brufatto N, Ward A, Nesheim ME (2003) Factor Xa is highly protected from antithrombin-fondaparinux and antithrombin-enoxaparin when incorporated into the prothrombinase complex. J Thromb Haemost 1: 1258–1263.
46. Medsafe (2010) Clexane® and Clexane® Forte. Available: http://www.medsafe.govt.nz/profs/datasheet/c/clexaneinj.pdf. Accessed 20 Oct 2010.
47. Ferreira CN, Vieira LM, Dusse LM, Reis CV, Amaral CF, et al. (2002) Evaluation of the blood coagulation mechanism and platelet aggregation in individuals with mechanical or biological heart prostheses. Blood Coagul Fibrinolysis 13: 129–134.
48. Eriksson BI, Borris L, Dahl OE, Haas S, Huisman MV, et al. (2006) Oral, direct Factor Xa inhibition with BAY 59-7939 for the prevention of venous thromboembolism after total hip replacement. J Thromb Haemost 4: 121–128.
49. Turpie AGG, Fisher WD, Bauer KA, Kwong LM, Irwin MW, et al. (2005) BAY 59-7939: an oral, direct factor Xa inhibitor for the prevention of venous thromboembolism in patients after total knee replacement. A phase II dose-ranging study. J Thromb Haemost 3: 2479–2486.
50. Eriksson BI, Borris LC, Dahl OE, Haas S, Huisman MV, et al. (2006) A once-daily, oral, direct Factor Xa inhibitor, rivaroxaban (BAY 59-7939), for thromboprophylaxis after total hip replacement. Circulation 114: 2374–2381.
51. Eriksson BI, Borris LC, Friedman RJ, Haas S, Huisman MV, et al. (2008) Rivaroxaban versus enoxaparin for thromboprophylaxis after hip arthroplasty. N Engl J Med 358: 2765–2775.
52. Kakkar AK, Brenner B, Dahl OE, Eriksson BI, Mouret P, et al. (2008) Extended duration rivaroxaban versus short-term enoxaparin for the prevention of venous thromboembolism after total hip arthroplasty: a double-blind, randomised controlled trial. Lancet 372: 31–39.
53. Lassen MR, Ageno W, Borris LC, Lieberman JR, Rosencher N, et al. (2008) Rivaroxaban versus enoxaparin for thromboprophylaxis after total knee arthroplasty. N Engl J Med 358: 2776–2786.
54. Turpie AGG, Lassen MR, Davidson BL, Bauer KA, Gent M, et al. (2009) Rivaroxaban versus enoxaparin for thromboprophylaxis after total knee arthroplasty (RECORD4): a randomised trial. Lancet 373: 1673–1680.
55. Agnelli G, Gallus A, Goldhaber SZ, Haas S, Huisman MV, et al. (2007) Treatment of proximal deep-vein thrombosis with the oral direct Factor Xa inhibitor rivaroxaban (BAY 59-7939): the ODIXa-DVT (oral direct Factor Xa inhibitor BAY 59-7939 in patients with acute symptomatic deep-vein thrombosis) study. Circulation 116: 180–187.
56. Buller HR, Lensing AW, Prins MH, Agnelli G, Cohen A, et al. (2008) A dose-ranging study evaluating once-daily oral administration of the Factor Xa inhibitor rivaroxaban in the treatment of patients with acute symptomatic deep vein thrombosis. The EINSTEIN-DVT Dose-Ranging Study. Blood 112: 2242–2247.
57. Haas S (2008) New oral Xa and IIa inhibitors: updates on clinical trial results. J Thromb Thrombolysis 25: 52–60.